Am J Cancer Res 2020;10(8):2510-2522
www.ajcr.us /ISSN:2156-6976/ajcr0102474

Original Article

GFPT2 promotes metastasis and forms a positive feedback loop with p65 in colorectal cancer

Lixin Liu[1*], Yangjian Pan[1*], Xiaoli Ren[2,3,4*], Zhicheng Zeng[2,3,4], Jingbo Sun[1], Kun Zhou[1], Yunshi Liang[2,3,4], Feifei Wang[2,3,4], Yongrong Yan[2,3,4], Wenting Liao[2,3,4], Yanqing Ding[2,3,4], Xiaolong Liu[1], Li Liang[2,3,4]

[1]Department of General Surgery, The Third Affiliated Hospital of Southern Medical University, Guangzhou 510515, Guangdong Province, People's Republic of China; [2]Department of Pathology, Nanfang Hospital, Southern Medical University, Guangzhou 510515, Guangdong Province, People's Republic of China; [3]Guangdong Province Key Laboratory of Molecular Tumor Pathology, Guangzhou 510515, Guangdong Province, People's Republic of China; [4]Department of Pathology, Basic Medical College, Southern Medical University, Guangzhou 510515, Guangdong Province, People's Republic of China. [*]Equal contributors and co-first authors.

Received September 18, 2019; Accepted April 7, 2020; Epub August 1, 2020; Published August 15, 2020

Abstract: As a rate-limiting enzyme of the hexosamine biosynthesis pathway (HBP), which is responsible for glycosylation, Glutamine fructose-6-phosphate amidotransferase 2 (GFPT2) is involved in human breast and lung tumorigenesis. However, whether GFTP2 is associated with tumor metastasis remains unclear. Here, we found that GFPT2 promoted the proliferation, migration, invasion and metastasis of colorectal cancer (CRC) cells. Mechanically, p65 acted as an upstream transcription factor of GFPT2 and regulated its expression and function. In turn, GFPT2 enhanced the glycosylation of p65, which led to the nuclear translocation of p65 and then activated NF-κB pathway. Thus, GFTP2 and p65 formed a positive feedback loop to promote the progression of CRC. In addition, GFPT2 was up-regulated in CRC tissues and closely related with liver metastasis (P<0.0001) and tumor stage (P=0.0184). High expression of GFPT2 predicted poor prognosis for CRC patients. Moreover, GFTP2 expression was positively linked with O-linked N-acetylglucosamine transferase in CRC tissues. Our study reveals a new mechanism of GFPT2 in CRC metastasis and provides a new target therapeutic target to deter metastasis.

Keywords: GFPT2, NF-κB pathway, p-65 glycosylation, metastasis, colorectal cancer

Introduction

Colorectal cancer (CRC) has become the third of the most common malignancies and its morbidity and mortality are rising [1]. Ample evidence indicate that metastasis is the main cause for CRC patients' deaths. Although the development of medical technology has been distinctly improved, 90% patients with malignant tumors will die of complications related to tumor metastasis [2]. Thus, it is necessary to clarify the molecular mechanisms during metastasis and discover novel treatment strategy for CRC patients.

Glutamine-fructose-6-phosphate transaminase (GFPT) is a rate-limiting enzyme of the hexosamine biosynthesis pathway (HBP), which is one of the most common and important ways in glucose metabolism and responsible for glycosylation [3]. GFPT can catalyze the formation of glucosamine-6-phosphate from glucosamine and fructose-6-phosphate, which is bypassed by glucosamine infusions [4]. GFPT is encoded by the unlinked highly homologous genes GFPT1 and GFPT2. Recent studies have suggested that the alteration of GFPT expression may result in hyperinsulinemia, obesity and insulin resistance [5-7]. GFPT2 is highly expressed in more aggressive breast cancer cell lines [8]. High expression of GFPT2 in cancer-associated fibroblasts increases the glucose uptake of human lung adenocarcinoma [9]. However, the function of GFPT2 in tumor metastasis remains still unclear. Our study shows that GFPT2 acts as an oncogene in proliferation and metastasis of CRC by activating the NF-κB pathway through positive feedback.

Materials and methods

Human specimens and cell lines

Paraffin-embedded CRC samples and fresh CRC tissues were collected from 85 patients who underwent CRC resection without prior radiotherapy and chemotherapy at the Department of General Surgery in Nanfang Hospital in 2011 year. Fresh CRC samples were collected immediately after resection, snap-frozen in liquid nitrogen, and then stored at -80°C. All patients were followed up for 5 years.

Human normal colon mucosal epithelial cell line SW460 and CRC cell lines SW480, SW620, HCT116, RKO, HT29 and LOVO were purchased from American Type Culture Collection (ATCC). All cell lines were cultured in 1640 medium (GIBCO, Gaithersburg, MD, USA) with 10% fetal bovine serum (HyClone, Logan, USA) at 37°C under 5% CO_2.

Construction of plasmids and transfection

For depletion of GFPT2, the lentivirus vectors carrying human shRNA (Genechen, Shanghai, China) was transfected into lentiviral packaging cell lines 293T cells. The shRNA sequence was follows: shRNA1 5'-GACCGAATTTCACTACAAA-3', shRNA2 5'-GGTTGAACTTGCTAGTGAT-3'. A scramble shRNA (5'-AAT CGC ATA GCG TAT GCC GTT-3'), which has no homology with the mammalian mRNA sequences, was inserted into empty lentivirus vector as described above. Then 1 mL of viral supernatant containing 4Ag of polybrene was added into GC cell lines for stable transduction. After 14 days, puromycin-resistant cell pools were established. After 72 h, the protein level of GFPT2 was detected by western blotting.

Subcutaneous tumor implantation and metastasis assays

Four-to-six-week-old male athymic BALB/c-nu/nu mice were purchased from the Central Laboratory of Animal Science at Southern Medical University (Guangzhou, China). All protocols for animal studies were reviewed and approved by the Institutional Animal Care and Use Committee in our University. Cells (1.5 million) were injected into the left and right flanks of nude mice for subcutaneous tumor implantation and allowed to grow for 28 days before mice were sacrificed. For metastasis assay, cells (0.5 million) were injected into cecum serosa and mice were sacrificed in 40 days. All tissues were embedded in paraffin, sectioned, stained with hematoxylin and eosin, or subjected to immunohistochemistry staining.

Co-Immunoprecipitation (Co-IP)

Cell lysis was incubated 2 h at 4°C with IgG and protein A+G Agarose to get rid of unspecific binding. NF-κB -p65 and O-GlcNAc antibodies were then added at 4°C overnight. The protein A/G-agarose was collected by centrifugation. Immuno-precipitated proteins were analyzed by SDS-PAGE (10%, Minigel) at 100 V for 1.5 h. NF-κB-p65 and O-GlcNAc antibodies were diluted, respectively and incubated with membranes at 4°C overnight. The secondary antibodies were then incubated for 1 h at room temperature. Protein bands were visualized using enhanced chemiluminescence (PerkinElmer Life Sciences).

Cell proliferation assay

1×10^3 cells were seeded into 96-well plates. The number of viable cells was determined by cell counting kit-8 (CCK-8) (Dojindo, Kumamoto, Japan) for 6 days. Briefly, 10 μL CCK-8 solution was added, and absorbance at 490 nm was measured after 2 h of incubation at 37°C. For plate colony assay, 800 cells were seeded into 6-well plates and cultured at 5% CO_2, 37°C for 2 weeks. Then we counted the number of colonies (each colony >50 cells) which were stained with hematoxylin. Each cell group was plated in 3 duplicate wells.

In vitro invasion assay

Boyden invasion chambers were rehydrated with RPMI 1640 (serum-free) for 2 hours at 37°C. RPMI 1640 with 100 ml/L fetal bovine serum was added to the lower compartments the chemotactic factor. Then 1.5×10^5 tumor cells in serum-free Dulbecco's modified Eagle medium were added to the upper compartment of the chamber. After incubation for 48 hours, the noninvasive cells were removed with a cotton swab. Cells that had migrated through the membrane and stuck to the lower surface of the membrane were stained with hematoxylin and counted under a light microscope in 5 random visual fields (200×). Each experiment was repeated 3 times.

Immunohistochemistry (IHC)

In brief, paraffin-embedded specimens were cut into 4 μm sections. The sections were deparaffinized with xylenes and rehydrated. Sections were submerged into EDTA antigenic retrieval buffer and microwaved for antigenic retrieval. The sections were treated with 3% hydrogen peroxide in methanol to quench the endogenous peroxidase activity, followed by incubation with 1% bovine serum albumin to block the nonspecific binding. Antibodies against GFPT2 (1:200), Ki-67 (1:1000) were incubated with the sections overnight at 4°C, respectively. After incubation with secondary antibody, the visualization signal was developed with 3,3'-diaminobenzidine tetrachloride (DAB). The stained tissue sections were reviewed and scored separately by two pathologists blinded to the clinical parameters. The total GFPT2 or Ki67 immunostaining score was calculated as the sum of the percent positivity of stained tumor cells and the staining intensity. The percent positivity was scored as "0," 0%; "1" 1-25%; "2" 26-50%; "3" 51-75% and "4" >75%. The staining intensity was scored as "0" (no staining), "1" (weakly stained), "2" (moderately stained) and "3" (strongly stained). Both percent positivity of cells and staining intensity were decided in a double blinded manner. The staining of gene was assessed as follows: (-) means a final staining score of <3; (+) a final staining score of 3; (+ +) a final staining score of 4; and (+ + +) a final staining score of ≥5. This relatively simple, reproducible scoring method gives highly concordant results between independent evaluators. An optimal cut off value was identified: Tumors with a final staining score 0~+ were classified as those with low expression of GFPT2, and tumors with a final staining score ++~+++ were classified as those with high expression of GFPT2.

RNA extraction and real-time RT-PCR

Total RNA was extracted using TRIzol reagent (Invitrogen, Carlsbad, CA, USA) and cDNA was synthesized by using an access reverse transcription system (Promega, Madison, WI, USA). The PCR primers for GFPT2 were as follows: Forward: 5'-ATG TGC GGA ATC TTT GCC TAC-3'; Reverse: 5'-ATC GAG AGC CTT GAC TTT CC C-3'. The first-strand cDNA was synthesized using the Prime Script RT reagent Kit (TaKaRa, Dalian, China). Real-time PCR was performed using SYBR Premix Ex Taq II (TaKaRa) and measured in a LightCycler 480 system (Roche, Basel, Switzerland). Expression of GAPDH was used as internal control. All the reactions were run in triplicate.

Western blotting

Protein lysates were prepared, subjected to SDS/PAGE, transferred onto PVDF membranes and blotted according to standard methods using anti-GFPT2 polyclonal antibody (1:500, Abcam, Cambridge, UK), NF-κB -p65 (1:500, Proteintech), O-GlcNAcase (OGA) (1:500, Proteintech), O-linked N-acetylglucosamine (GlcNAc) transferase (OGT) (1:500, Proteintech), p-IKB-α (1:300, abcam) and O-GlcNAc (1:200, Proteintech). A mouse monoclonal anti-GAPDH (1:1000) (Sigma-Aldrich, St. Louis, USA) or β-actin antibody (1:1000) (Sigma-Aldrich, St. Louis, USA) or Histone H3 (1:500, Sigma-Aldrich, St. Louis, USA) was used as inner control to confirm equal loading of proteins.

Statistical analysis

Expression of GFPT2 in CRC tissues was analyzed with Wilcoxon Signed Ranks Test. The correlation of GFPT2 expression to various clinicopathological parameters was evaluated with chi-suqare test. Survival analyses were performed according to the Kaplan-Meier method and compared by the log-rank test. Cell proliferation and in vitro invasion assay were tested using one-way ANOVA. All statistical analyses were analyzed using the SPSS 20.0 software and $P<0.05$ was considered significant.

Results

GFPT2 promotes the proliferation, migration, invasion and metastasis of CRC cells

To explore the function of GFPT2 in CRC progression, gain-of and loss-of-function experiments of GFPT2 were performed using ectopic plasmids or shRNA fragments. Based on the endogenous GFPT2 expression in CRC cell lines (Figure S1A, S1B), we over-expressed GFPT2 in SW480 cells and down-regulated GFPT2 in SW620 cells (Figure S1C, S1D). Results of CCK-8 assays exhibited that ectopic GFTP2 increased the proliferative abilities of SW480 cells (**Figure 1A**). Conversely, knockdown of GFPT2 in SW620 cells showed decreased pro-

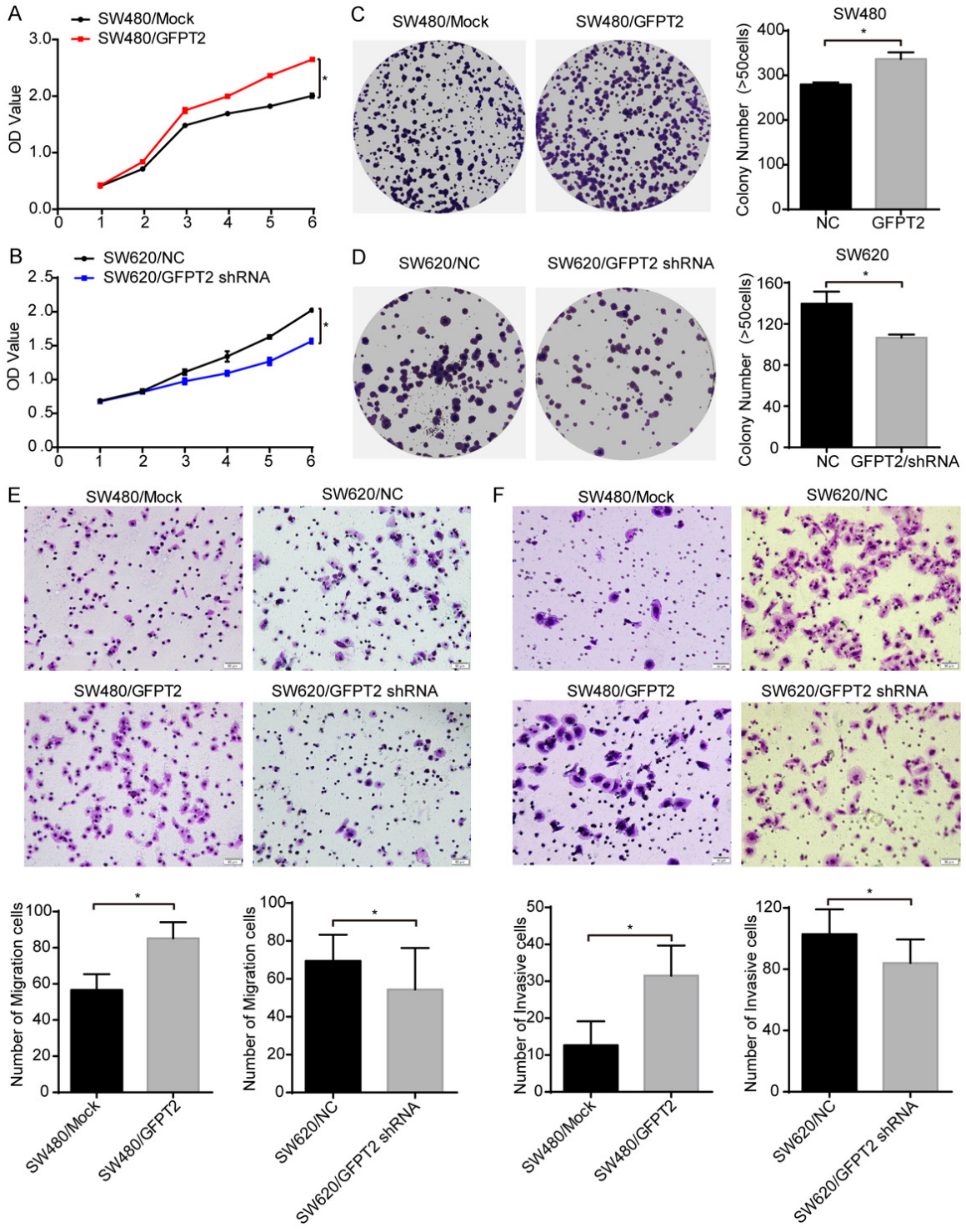

Figure 1. GFPT2 promoted proliferation, migration and invasion of CRC cells in vitro. A, B. Effect of GFPT2 overexpression or down regulation on cell proliferation of SW480 or SW620 cells detected by CCK-8 assay. C, D. Effect of GFPT2 overexpression or inhibition on cell clone formation ability of SW480 and SW620 cells. E. Effect of GFPT2 overexpression or inhibition on cell migration of SW480 and SW620 cells. F. Effect of GFPT2 overexpression or inhibition on cell invasion of SW480 and SW620 cells. Error bars represent mean ± SD from three independent experiments. *P<0.05.

liferative abilities (**Figure 1B**). Similarly, enhanced GFPT2 in SW480 cells obviously increased the colony number compared with control group (**Figure 1C**, P<0.05), while inhibi-

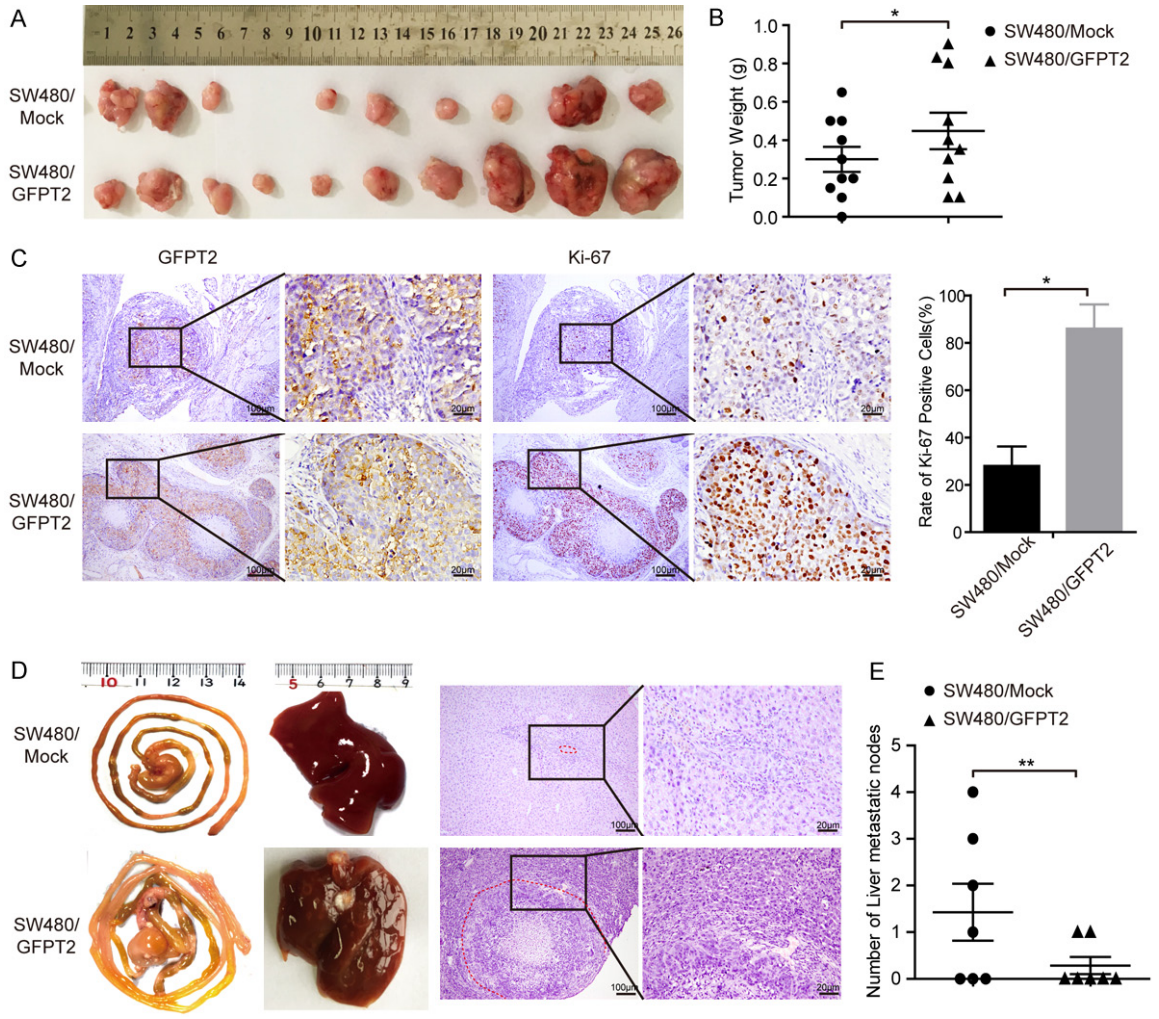

Figure 2. GFPT2 promoted proliferation and metastasis of CRC cells in vivo. A. Images and statistical analysis of subcutaneous tumor formed by SW480/Mock or SW480/GFPT2 cells. B. Qualification of tumor weight in SW480/Mock or SW480/GFPT2 groups. C. Representative images of Ki67 staining in subcutaneous tumor sections by immunohistochemistry. D. The effect of GFPT2 overexpression on metastasis in SW480 cells. E. Qualification of metastatic nodes in mice liver in SW480/Mock or SW480/GFPT2 groups. Scale bars: 100 μm or 20 μm. Error bars represent mean ± SD from three independent experiments. *P<0.05.

tion of GFPT2 in SW620 cells showed the opposite results (**Figure 1D**, P<0.05). Moreover, over-expression of GFPT2 displayed a marked increase of migratory and invasive abilities in SW480 cells, while depletion of GFPT2 had the opposite effect (**Figure 1E**, **1F**, P<0.05). In addition, we implanted GFPT2-expressing cells and control cells subcutaneously into nude mice respectively, and then monitored the growth of the resultant primary tumors. Tumors in mice injected with GFPT2-expressing cells grew more rapidly than control group (**Figure 2A**, **2B**). We selected five obviously different paired groups of tumors for Ki-67 detection. IHC staining confirmed that GFPT2 expressing tumors displayed much higher positive Ki-67 percentages than control group (**Figure 2C**). Anymore, we also knocked down the expression of GFPT2 in SW620 cell line in vivo assays and results showed that tumors in GFPT2 knock-down group displayed larger volume and lower positive Ki-67 percentages than NC group (Figure S2A, S2B). We also examined the effect of GFPT2 on CRC metastasis in vivo. Cells were transplanted into the cecum of nude mice, with the results that the number of liver metastases in SW480/GFPT2 group was obviously increased (**Figure 2D**, **2E**, P<0.05). These results make it evident that GFPT2 is a positive regulator of CRC progression.

P65 transcriptionally regulates GFPT2 to promote proliferation and invasion in CRC cells

Having confirmed the tumor promoting role of GFPT2 in CRC, we set out to explore the molecular mechanisms of its function. Both Gene Set Enrichment Analysis (GSEA) and JASPAR online biotechnology tool predicted the transcription factor NF-κB-p65 as a potential interacting factor with GFPT2 (**Figure 3A**). Transient transfection of both p65 and GFPT2 promoter could significantly increase the luciferase activity of SW480 cells. On the contrary, transfection of p65 or GFPT2 promoter alone or both p65 and the mutant of GFPT2 promoter did not affect the luciferase activity (**Figure 3B**, $P<0.05$). Moreover, ectopic p65 increased both mRNA and protein levels of GFPT2, depletion of p65 presented the adverse effects (**Figures 3C**, S1E and S1F, $P<0.05$). Over-expression of p65 accelerated the proliferation and invasion of SW480 cells, while simultaneous depletion of GFPT2 at least partially reversed p65-induced cell proliferation and invasion in vitro (**Figure 3D**, **3F**). Contrarily, knockdown of p65 reduced the proliferation and invasion of SW620 cells, while reintroduction of GFPT2 rescued the suppression induced by p65 knockdown (**Figure 3E**, **3G**). These results indicate that p65 acts as a upstream transcriptional factor of GFPT2 to promote the proliferation and invasion of CRC cells.

GFPT2 activates NF-κB pathway via up-regulation of the glycosylation of p65 to promote invasion and metastasis of CRC

Recent evidence shows that HBP is strongly linked with aberrant glycosylation in tumors. Alterations of UDP-GlcNAc and its derivates, the substrate donors such as O-GlcNAcylation, proteoglycan produced by HBP way can lead to abnormal glycosylation [3, 10, 11]. Although as a key rate-limiting enzyme of HBP, the role of GFPT2 in glycosylation of CRC seldom reported. Our results showed that up-regulation of GFPT2 in SW480 cells enhanced the levels of O-GlcNAc and OGT, not O-GlcNAcase (OGA). While depletion of GFPT2 in SW620 cells showed the opposite effect (**Figure 4A**). HBP is responsible for the glycosylation and NF-κB pathway can be activated by O-GlcNAc glycosylation [12-15]. But whether GFPT2 regulates the glucosylation of p65 is still unknown. Co-IP assays showed that exogenous p65 bound with O-GlcNAcylation in SW480 cells (**Figure 4B**). Enforced expression of GFPT2 promoted the binding of p65 with O-GlcNAcylation (**Figure 4B**). Meanwhile, up-regulation of GFPT2 did not change the total level of p65, but significantly accelerated the nuclear translocation of p65 (**Figure 4C**), while the treatment of O-GlcNAcylation inhibitor Benzyl-d-GlcNAc reversed the effect (**Figure 4D**, **4E**). Furthermore, Benzyl-d-GlcNAc treatment decreased the proliferation, migration and invasion of SW480 cells induced by GFPT2 (**Figure 4F-I**). These data demonstrate that GFPT2 activates NF-κB pathway via O-GlcNAcylation of p65 in CRC cells, hence forming a positive feedback loop between GFTP2 and p65.

GFPT2 is up-regulated in CRC and predicts poor prognosis for CRC patients

To assess the expression pattern of GFTP2 and its clinicopathologic value in CRC, we detected the mRNA level of GFTP2 in 30 cases of fresh CRC tissues. The mRNA level of GFPT2 was significantly higher in CRC tissues than the matched normal mucosa (**Figure 5A**, **5B**). And the expression of GFPT2 in CRC tissues with metastasis was higher than those without metastasis (**Figure 5C**). We then analyzed GFPT2 expression in 85 cases of paraffin-embedded archived CRC tissues by IHC. Strong staining for GFPT2 protein was frequently observed in CRC tumors, especially in lymphatic and liver metastases (**Figure 5D**). The expression of GFPT2 was up-regulated in CRC tissues compared with normal mucosa and significantly gradually increased in primary tumor, lymphatic and liver metastasis (**Figure 5E**). Moreover, GFTP2 expression was closely related with tumor stage (**Figure 5F**). Clinicopathological analyses showed that GFPT2 expression was correlated strongly with liver metastasis and tumor stage ($P<0.0001$, $P=0.0184$, respectively, **Table 1**). Kaplan Meier survival analysis showed a significant poorer survival in CRC patients with GFPT2 high expression (**Figure 5G**, $P<0.001$). The above results indicate that up-regulation of GFPT2 is associated with CRC metastasis and can be an independent prognostic marker for survival of CRC patients.

A

Table:GSEA Results Summary

Dataset	GFPT2_collapsed _to_symbols.chip.cls#H_versus_L
Phonotypc	chip.cls#H_versus_L
Uprogulated in clase	H
Gene Set	HALLMARK_TNFA_SIGNALING_VIA_NF-κB
Enrichment Score (ES)	0.6950711
Normalized enrichment score (NES)	2.0143209
Nominal p-value	0.0
FDR q-value	0.005034647
FWER p-value	0.025

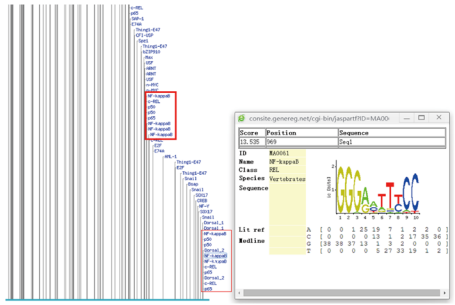

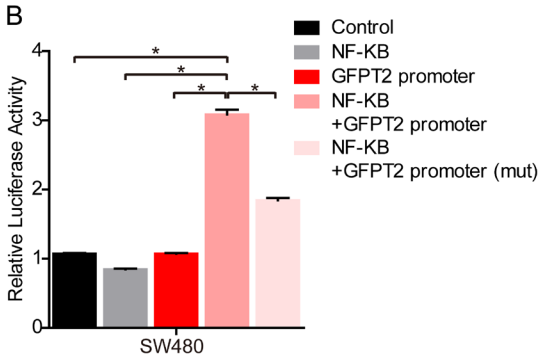

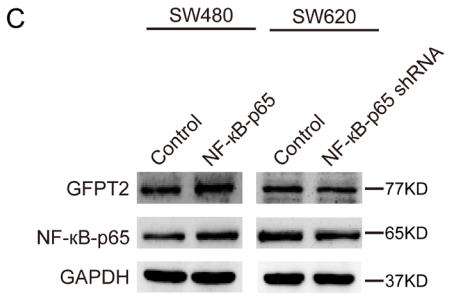

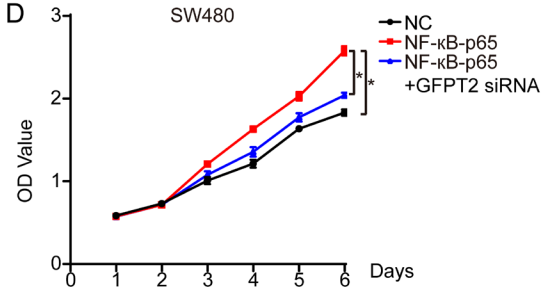

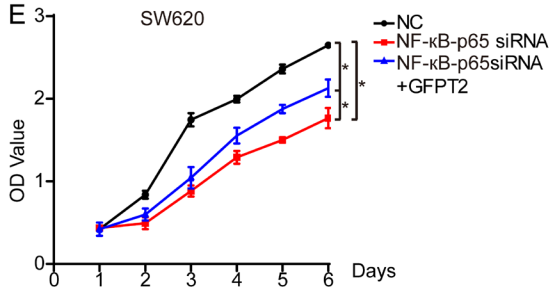

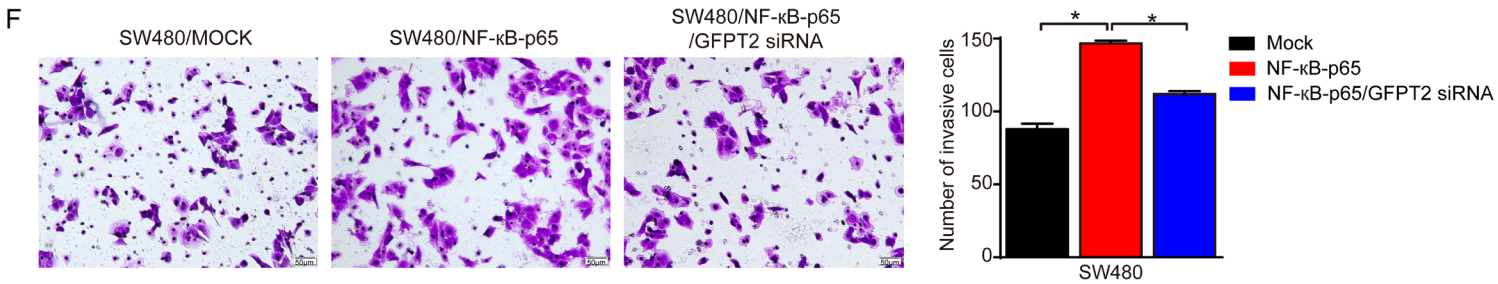

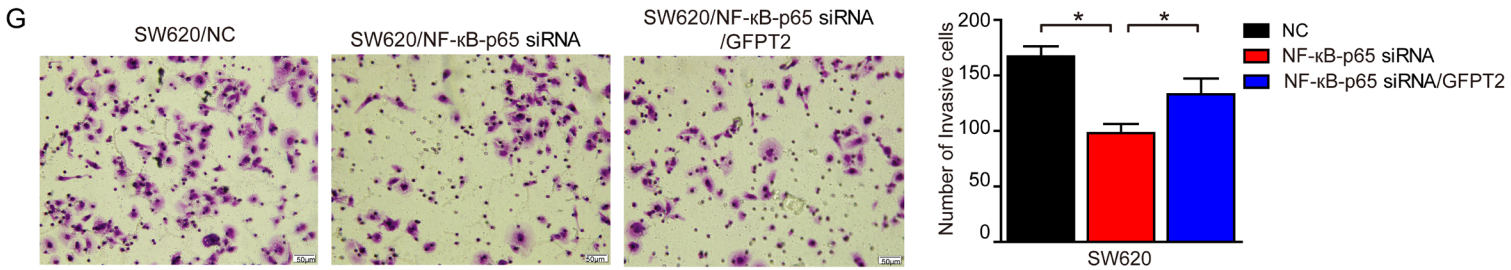

Figure 3. Up-stream transcription factor NF-κB-P65 regulates GFPT2 to promote proliferation, migration and invasion in CRC cells. A. Signal pathway enrichment in the condition of GFPT2 overexpression using gene set enrichment analysis in GSEA13294. B. Detection of combination of NF-κB-P65 and GFPT2 promoter by dual-luciferase report assay. C. The effect of NF-κB-P65 on the regulation of GFPT2 protein levels by Western blot. GAPDH was used as internal control. D-G. The rescue effect of GFPT2 in SW480/NF-κB-P65 or SW620/NF-κB-P65 siRNA cells on proliferation, migration or invasion by CCK8 and transwell assays. Scale bars: 20 μm. Error bars represent mean ± SD from three independent experiments. *P<0.05.

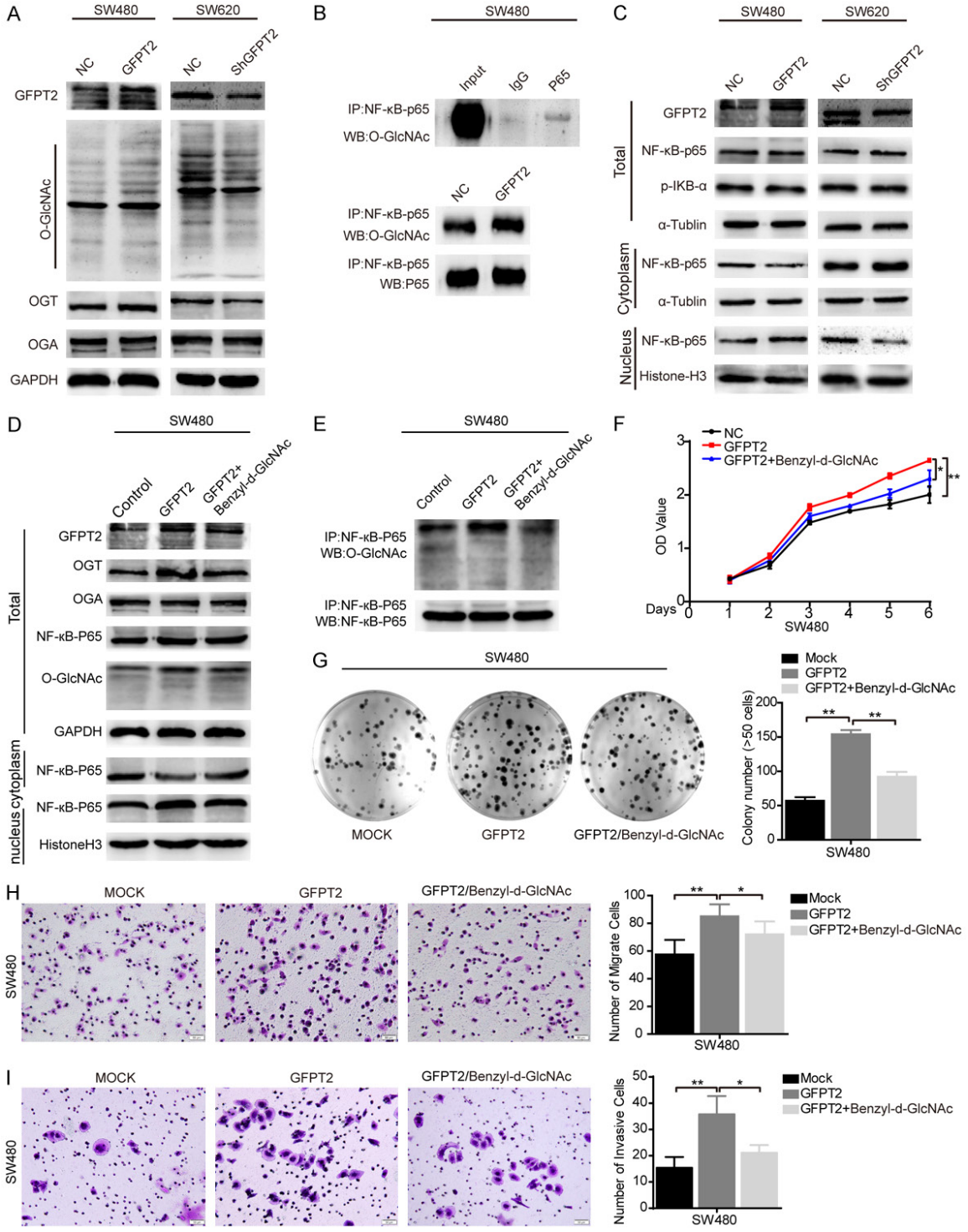

Figure 4. GFPT2 positively feedback activates NF-κB pathway via up-regulation of the glycosylation of p65 to promote invasion and metastasis of colorectal cancer. A. The effect of GFPT2 on glycosylation relative proteins: OGA, OGT, O-GlcNAc by Western blot. B. Combination between NF-κB-P65 and O-GlcNAc in SW480 cells by CoIP assay. C. The effect of GFPT2 on activating NF-κB pathway in SW480 and SW620 cells by Western blot. D. The rescue effect of Benzyl-d-GlcNAc on NF-κB-P65 nuclear translocation in SW480/GFPT2 cells. E. The rescue effect of Benzyl-d-GlcNAc on NF-κB-P65 glycosylation in SW480/GFPT2 cells. F-I. The rescue effect of Benzyl-d-GlcNAc on proliferation, migration or invasion by CCK8, plate clone and transwell assays in SW480/GFPT2 cells. Scale bars: 20 μm. Error bars represent mean ± SD from three independent experiments. *P<0.05.

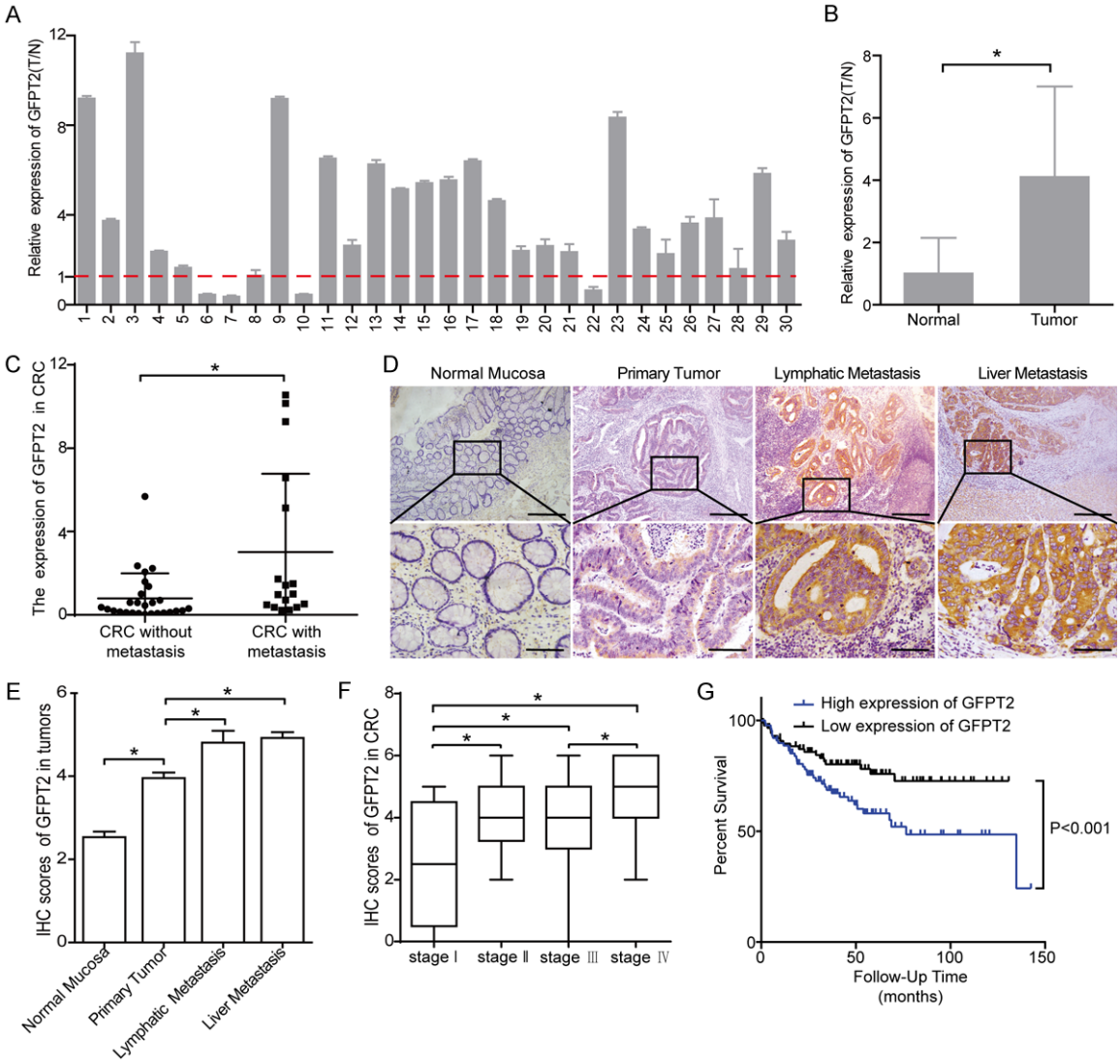

Figure 5. GFPT2 is up-regulated in CRC and predicts poor prognosis for CRC patients. A, B. Qualification of GFPT2 mRNA level in 30 cases of fresh CRC tissues and corresponding normal mucosa by qPCR. C. Relative mRNA level of GFPT2 in CRC tissues with or without metastasis. D. Representative images of GFPT2 proteins in 85 cases of paraffin-embedded CRC specimens by immunohistochemistry. E. Analyses of GFPT2 expression in normal tissue, primary tissue, lymphatic metastases or liver metastases by IHC. F. Analyses of GFPT2 expression in CRC tissues with different clinical stages. G. High expression of GFPT2 associated with shorter survival of CRC patients by Kaplan-Meier analysis. Error bars represent mean ± SD from three independent experiments. *P<0.05.

Expression of GFPT2 and OGT is highly linked in CRC tissues

Finally, we analyzed the expression correlations of GFPT2 with OGT in CRC tissues. IHC results displayed that there was positive relationship between GFPT2 and OGT in 30 paraffin samples (r=0.5794, P=0.0024, **Figure 6A**). In 21 cases fresh CRC tissues, there was a significant correlation between GFPT2 and OGT

Table 1. Relationship between GFPT2 expressions and clinicopathologic features of CRC patients

Features	Total no.	High expression	Low expression	*P* value
All cases	85	36	49	
Age (y)				0.3953
≥50	58	28	24	
<50	27	9	12	
Sex				0.1715
Male	63	29	23	
Female	22	8	13	
Differentiation				0.3852
Well	39	14	17	
Moderate	34	21	14	
poor	12	2	5	
Tumor stage				0.0184
T1-3	48	21	40	
T4	24	15	9	
Liver Metastasis				<0.0001
Yes	34	25	9	
No	51	11	40	
Lymph node metastasis				0.1394
Yes	41	14	27	
No	44	22	22	
Tumor size (cm)				0.0852
<5	56	20	36	
≥5	29	16	13	

(R^2=0.2428, P=0.0232, **Figure 6B**, **6C**). Moreover, GFTP2 expression was positively correlated with OGT in GTFP2 expressing subcutaneous tumors (**Figure 6D**). These results indicate that GFPT2 and OGT expression is highly linked in CRC tissues.

Discussion

As a rate-limiting enzyme of HBP, there is no doubt that GFPT2 plays important roles in cell life activities, especially in cell glucose metabolism [4]. Some studies have shown that GFPT2 might be associated with cancers including lung adenocarcinoma [9], breast cancer [8]. However, relatively little is known about the function of GFPT2 in tumorigenesis of CRC. Our data showed that high expression of GFPT2 in CRC tissues was closely related to poor prognosis of patients. Consistent with that, GFPT2 promoted the proliferation, invasion and metastasis of CRC cells, indicating that GFPT2 plays a promoting role in CRC progression.

NF-κB signaling pathway is involved in many tumors' proliferation, invasion and metastasis. As a member of NF-κB family, p65 can up-regulate the transactivation of target genes of diverse activities such as the cellular proliferation, inflammatory cytokines, chemokines, mediators of apoptosis and immunity [16-19]. Here, we verified that NF-κB-p65 acted as an upstream transcription factor of GFPT2 and promoted CRC cells proliferation, invasion and metastasis by regulating the expression of GFPT2.

Glycosylation is one of the major ways of protein modification after translation and plays an important role in life activities such as cellular immune regulation, protein translation and degradation [20]. Glycosylation modification is also involved in a variety of metabolic diseases and tumor development. In different tumor, abnormal glycosylation can affect tumor growth [21], epithelial to mesenchymal transition [22], tumor metastasis [23]. HBP is closely related to tumor glycosylation modification. Alterations of metabolites in HBP such as UDP-GlcNAc, O-GlcNAcylation, protein polysaccharide, glycolipid complex can induce abnormal glycosylation [24, 25]. In our study, we observed that up-regulation of GFPT2 could increase the expression of OGT and O-GlcNAcylation, not OGA. OGT plays an important role during the transfer of GlcNAc to the serine or threonine residues. On the contrary, O-GlcNAcase (OGA) removes O-GlcNAc from proteins [21, 26]. All the above data verify that GFPT2 is involved in the regulation of glycosylation in CRC.

When the canonical NF-κB signaling pathway is activated, phosphorylation of two important Serine site in IκB protein induces IκB phosphorylation and degradation. And then NF-κB proteins entered nuclear to bind with target genes such as TNF-α, IL-6 and initiate their transcription [27]. NF-κB signaling pathway can also be activated by O-GlcNAcylation. O-GlcNAcylation mediates NF-κB-p65 to affect the activity of NF-κB signal pathway [28]. It also activates the transcriptional function of NF-κB-c-Rel [29]. A

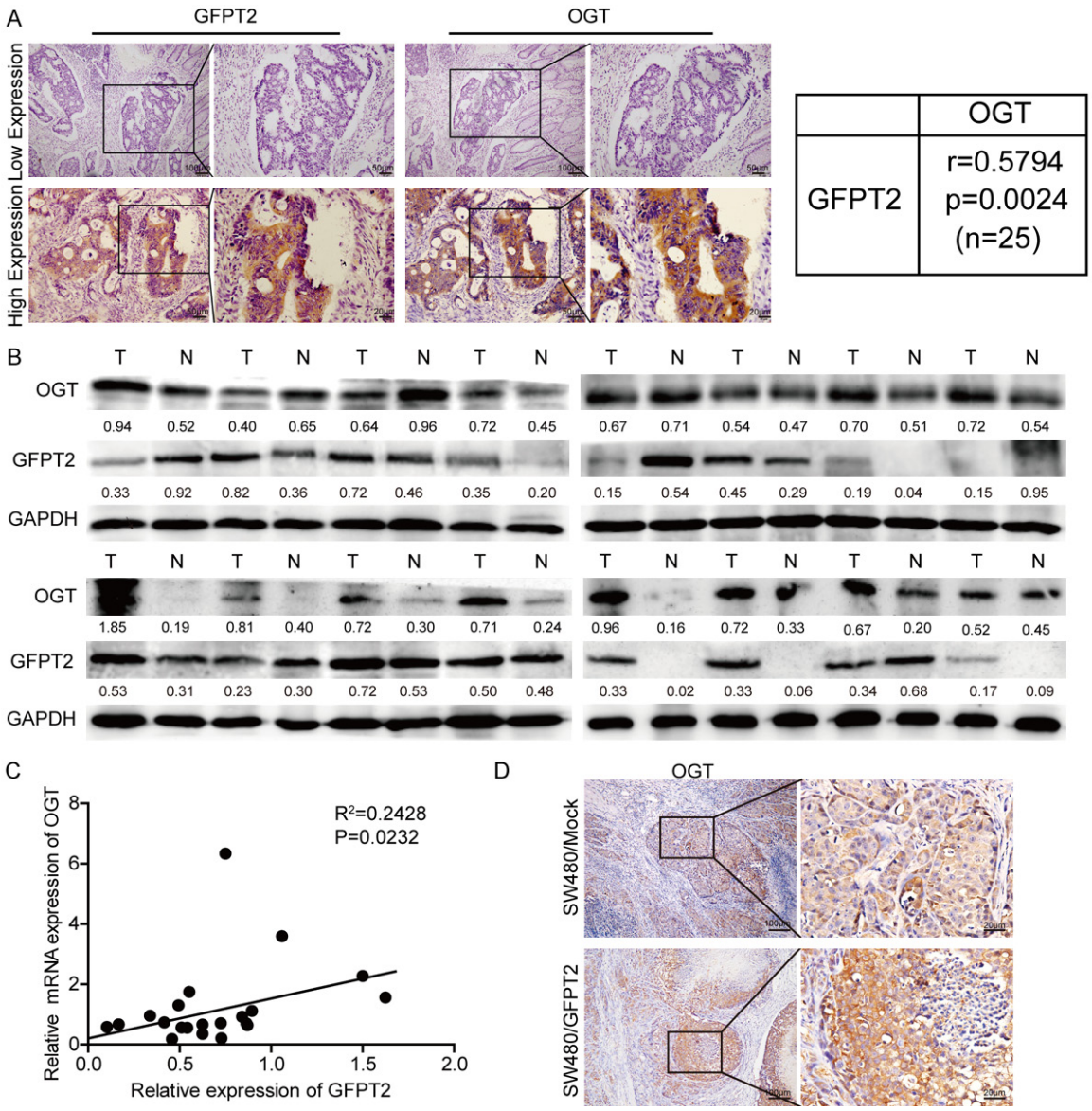

Figure 6. Expression of GFPT2 and OGT are highly linked in CRC tissues. A. Analyses of GFPT2 and OGT in 30 cases of paraffin-embedded CRC specimens by immunohistochemistry. B. Detection of OGT in 21 paired fresh CRC tissues by Western blot. C. The relationship of protein levels between GFPT2 and OGT in 21 cases of fresh CRC tissues. D. Detection of OGT expression in subcutaneous tumor sections.

series of studies have reported that NF-κB- p65 is usually O-GlcNAcylated on the serine or threonine residue such as Thr-352, Thr-322 or Ser 536 [30, 31]. High level of O-GlcNAcylation and NF-κB sustained activation are closely associated with pancreatic cancer [32]. But whether GFPT2 regulates O-GlcNAcylation of NF-κB in CRC is unknown. Our study revealed that GFPT2 mediated the glycosylation of NF-κB-p65. Benzyl-d-GlcNAc, an O-GlcNAcylation inhibitor, effectively blocked the influence of GFPT2 in glycosylation of NF-κB-p65.

Finally, we explored the expression associations between GFPT2 and OGT in CRC tissues. We found that the expression of GFPT2 was highly associated with OGT in CRC tissues. OGT was highly expressed in the human breast cancer, lung cancer, liver cancer, colorectal cancer, prostate cancer, etc. It is also involved in epithelial-mesenchymal transition (EMT) [33], metastasis, proliferation [34], drug resistance [35] of tumors. Our clinical data further validated the high links between GFTP2 and O-GlcNAcylation of P65 in CRC.

In conclusion, we present that NF-κB-p65 transcriptionally up-regulates GFPT2, in turn, GFPT2 enhances the glycosylation of NF-κB-p65, thus forming a positively feedback with p65, to promote CRC proliferation and metastasis. Our study reveals a new mechanism of GFPT2 in the progress of CRC.

Acknowledgements

This work was supported by the National key R&D program of China (2017YFC1309002), National Basic Research Program of China (973 Program, 2015CB554002), National Natural Science Foundation of China (81672821, 81773101, 81802306), Project funded by China Postdoctoral Science Foundation (2018M633081, 2018M633079), Natural Science Foundation of Guangdong Province (2018A030310457).

Disclosure of conflict of interest

None.

Address correspondence to: Xiaolong Liu, Department of General Surgery, The Third Affiliated Hospital of Southern Medical University, 183 West Zhongshan Avenue, Guangzhou 510630, Guangdong Province, People's Republic of China. Tel: +86-020-62784430; E-mail: lxl1979@i.smu.edu.cn; Li Liang, Department of Pathology, Southern Medical University, Guangzhou 510515, Guangdong Province, People's Republic of China. Tel: +86-020-62789099; E-mail: lli@fimmu.com

References

[1] Siegel RL, Miller KD and Jemal A. Cancer statistics, 2018. CA Cancer J Clin 2018; 68: 7-30.

[2] Gu MJ, Huang QC, Bao CZ, Li YJ, Li XQ, Ye D, Ye ZH, Chen K and Wang JB. Attributable causes of colorectal cancer in China. BMC Cancer 2018; 18: 38.

[3] Ruan HB, Singh JP, Li MD, Wu J and Yang X. Cracking the O-GlcNAc code in metabolism. Trends Endocrinol Metab 2013; 24: 301-309.

[4] Marshall S, Bacote V and Traxinger RR. Discovery of a metabolic pathway mediating glucose-induced desensitization of the glucose transport system: role of hexosamine biosynthesis in the induction of insulin resistance. J Biol Chem Chem 1991; 266: 4706-4712.

[5] Rvinen HY, Daniels MC, Ki AV, Mäkimattila S, DeFronzo RA and McClain D. Increased glutamine: fructose-6-phosphate amidotransferase activity in skeletal muscle of patients with NIDDM. Genomics 1996; 45: 302-307.

[6] Veerababu G, Tang J, Hoffman RT, Daniels MC, Hebert LF Jr, Crook ED, Cooksey RC and McClain DA. Overexpression of glutamine: fructose-6-phosphate amidotransferase in the liver of transgenic mice results in enhanced glycogen storage, hyperlipidemia, obesity, and impaired glucose tolerance. Diabetes 2000; 49: 2070-2078.

[7] Tang J, Neidigh JL, Cooksey RC and McClain DA. Transgenic mice with increased hexosamine flux specifically targeted to β-cells exhibit hyperinsulinemia and peripheral insulin resistance. Diabetes 2000; 49: 1492-1499.

[8] Simpson NE, Tryndyak VP, Beland FA and Pogribny IP. An in vitro investigation of metabolically sensitive biomarkers in breast cancer progression. Breast Cancer Res Treat 2012; 133: 959-68.

[9] Zhang W, Bouchard G, Yu A, Shafiq M, Jamali M, Shrager JB, Ayers K, Bakr S, Gentles AJ, Diehn M, Quon A, West RB, Nair V, van de Rijn M, Napel S and Plevritis SK. GFPT2-expressing cancer-associated fibroblasts mediate metabolic reprogramming in human lung adenocarcinoma. Cancer Res 2018; 78: 3445-3457.

[10] Zhang H, Jia Y, Cooper JJ, Zhang Z and Elbein SC. Common variants in glutamine: fructose-6-phosphate amidotransferase 2 (GFPT2) gene are associated with type 2 diabetes, diabetic nephropathy, and increased GFPT2 mRNA levels. J Clin Endocrinol Metab 2004; 89: 748-755.

[11] Wise DR and Thompson CB. Glutamine addiction: a new therapeutic target in cancer. Trends Biochem Sci 2010; 35: 427-433.

[12] Rumberger JM, Wu T, Hering MA and Marshall S. Role of hexosamine biosynthesis in glucose-mediated up-regulation of lipogenie cazyme mRNA levels: effects of glucose, glutamine and glucosamine on glycerophosphate dehydrogenase, fatty acid synthase and acetyl-CoA carboxylase mRNA levels. J Biol Chem 2003; 278: 28547-28552.

[13] Lynch TP, Ferrer CM, Jackson SR, Shahriari KS, Vosseller K and Reginato MJ. Critical role of O-Linked β-N-acetylglucosamine transferase in prostate cancer invasion, angiogenesis, and metastasis. J Biol Chem 2012; 287: 11070-11081.

[14] Itkonen HM, Minner S, Guldvik IJ, Sandmann MJ, Tsourlakis MC, Berge V, Svindland A, Schlomm T and Mills IG. O-GlcNAc transferase integrates metabolic pathways to regulate the stability of c-MYC in human prostate cancer cells. Cancer Res 2013; 73: 5277-5287.

[15] Mi W, Gu Y, Han C, Liu H, Fan Q, Zhang X, Cong Q and Yu W. O-GlcNAcylation is a novel regulator of lung and colon cancer malignancy. Biochim Biophys Acta 2011; 1812: 514-519.

[16] Basak S, Behar M and Hoffmann A. Lessons from mathematically modeling the NF-κB pathway. Immunol Rev 2012; 246: 221-238.
[17] Baldwin AS. Regulation of cell death and autophagy by IKK and NF-κB: critical mechanisms in immune function and cancer. Immunol Rev 2012; 246: 327-345.
[18] Yde P, Mengel B, Jensen MH, Krishna S and Trusina A. Modeling the NF-κB mediated inflammatory response predicts cytokine waves in tissue. BMC Syst Biol 2011; 5: 115.
[19] Sun S. The non-canonical NF-κB pathway in immunity and inflammation. Nat Rev Immunol 2017; 17: 545-558.
[20] Apweiler R, Hermjakob H and Sharon N. On the frequency of protein glycosylation, as deduced from analysis of the SWISS-PROT database. Biochim Biophys Acta 1999; 1473: 4-8.
[21] Slawson C and Hart GW. O-GlcNAc signalling: implications for cancer cell biology. Nat Rev Cancer 2011; 11: 678-684.
[22] Guan F, Handa K and Hakomori SI. Specific glycosphingolipids mediate epithelial-to-mesenchymal transition of human and mouse epithelial cell lines. Proc Natl Acad Sci U S A 2009; 106: 7461-7466.
[23] Häuselmann I and Borsig L. Altered tumor-cell glycosylation promotes metastasis. Front Oncol 2014; 4: 28.
[24] Alisson-Silva F, Freire-de-Lima L, Donadio JL, Lucena MC, Penha L, Sá-Diniz JN, Dias WB and Todeschini AR. Increase of O-glycosylated oncofetal fibronectin in high glucose-induced epithelialmesenchymal transition of cultured human epithelial cells. PLoS One 2013; 8: e60471.
[25] Dennis JW, Nabi IR and Demetriou M. Metabolism, cell surface organization, and disease. Cell 2009; 139: 1229-1241.
[26] Fardini Y, Dehennaut V, Lefebvre T and Issad T. O-GlcNAcylation: a new cancer hallmark? Front Endocrinol (Lausanne) 2013; 4: 99.
[27] Lai JL, Liu YH, Liu C, Qi MP, Liu RN, Zhu XF, Zhou QG, Chen YY, Guo AZ and Hu CM. Indirubin inhibits LPS-induced inflammation via TLR4 abrogation mediated by the NF-kB and MAPK signaling pathways. Inflammation 2017; 40: 1-12.
[28] Allison DF, Wamsley JJ, Kumar M, Li D, Gray LG, Hart GW, Jones DR and Mayo MW. Modification of RelA by O-linked N-acetylglucosamine links glucose metabolism to NF-κB acetylation and transcription. P Natl Acad Sci USA 2012; 109: 16888-16893.
[29] Ramakrishnan P, Clark PM, Mason DE, Peters EC, Hsieh-Wilson LC and Baltimore D. Activation of the transcriptional function of the NF-κB protein c-Rel by O-GlcNAc glycosylation. Sci Signal 2013; 6: ra75.
[30] Ma Z, Vocadlo DJ and Vosseller K. Hyper-O-GlcNAcylation is anti-apoptotic and maintains constitutive NF-κB activity in pancreatic cancer cells. J Biol Chem 2013; 288: 15121-15130.
[31] Ali A, Kim SH, Kim MJ, Choi MY, Kang SS, Cho GJ, Kim YS, Choi JY and Choi WS. O-GlcNAcylation of NF-κB promotes lung metastasis of cervical cancer cells via upregulation of CXCR4 expression. Mol Cells 2017; 40: 476-484.
[32] Xing D, Gong K, Feng W, Nozell SE, Chen YF, Chatham JC and Oparil S. O-GlcNAc modification of NF-kappa B p65 inhibits TNF-alpha-induced inflammatory mediator expression in rat aortic smooth muscle cells. PLoS One 2011; 6: e24021.
[33] Gao J, Yang Y, Qiu R, Zhang K, Teng X, Liu R and Wang Y. Proteomic analysis of the OGT interactome: novel links to epithelial-mesenchymal transition and metastasis of cervical cancer. Carcinogenesis 2018; 39: 1222-1234.
[34] Wang L, Chen S, Zhang Z, Zhang J, Mao S, Zheng J, Xuan Y, Liu M, Cai K, Zhang W, Guo Y, Zhai W and Yao X. Suppressed OGT expression inhibits cell proliferation while inducing cell apoptosis in bladder cancer. BMC Cancer 2018; 18: 1141.
[35] Zhou F, Yang X, Zhao H, Liu Y, Feng Y, An R, Lv X, Li J and Chen B. Down-regulation of OGT promotes cisplatin resistance by inducing autophagy in ovarian cancer. Theranostics 2018; 8: 5200-5212.

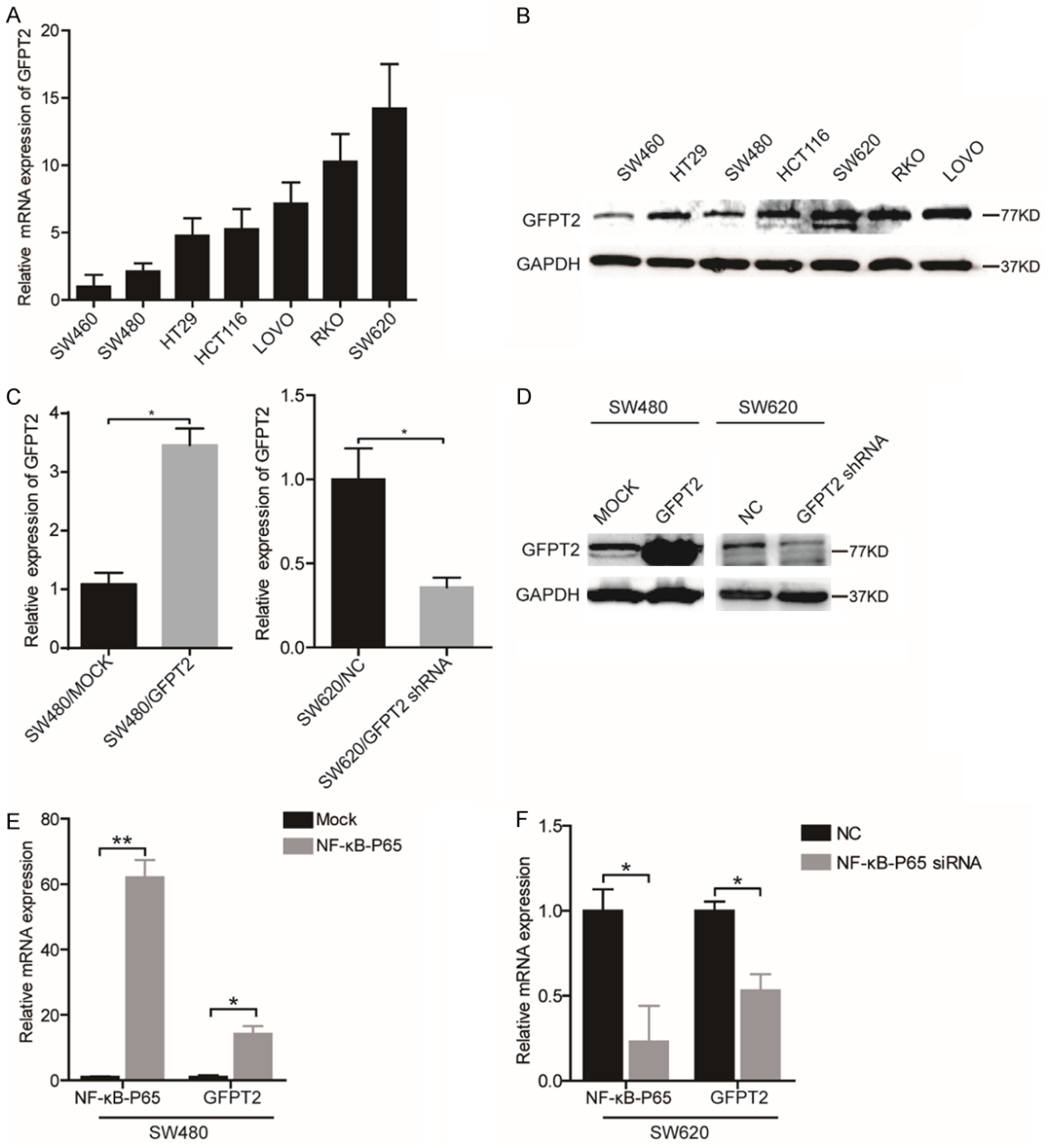

Figure S1. Endogenous expression and efficiency of GFPT2 transfection in CRC cells. (A, B) Endogenous expression of GFPT2 mRNA (A) and protein (B) in human CRC cells by qPCR and Western blot. (C, D) Relative mRNA (C) and protein (D) expressions of GFPT2 in SW480 and SW620 cells by qPCR and Western blot. (E, F) Relative mRNA expressions of GFPT2 and NF-κB-P65 in SW480 and SW620 cells transiently transfected with NF-κB-P65 vector or shRNAs by qPCR.

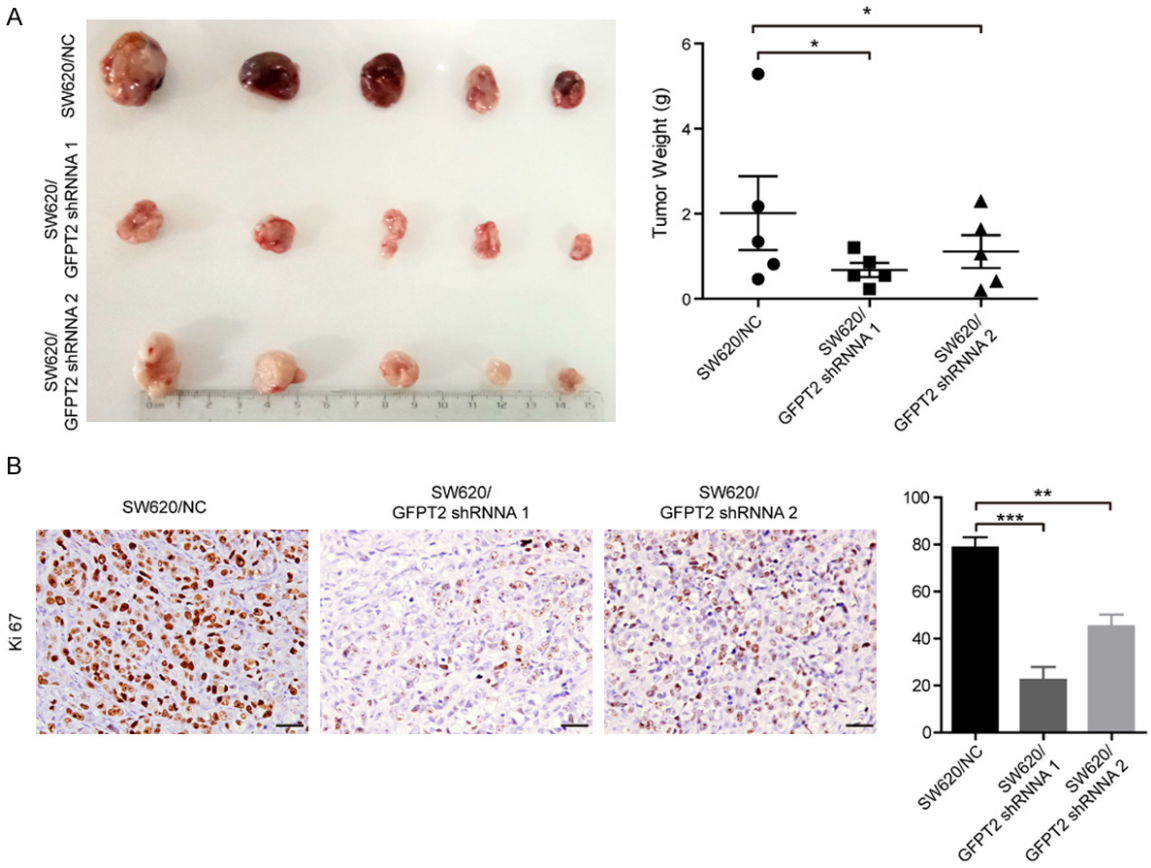

Figure S2. Down-regulation of GFPT2 inhibit proliferation of CRC cells in vivo. A. Images and statistical analysis of subcutaneous tumor formed by SW620/NC or SW620/GFPT2 shRNA1 or SW480/GFPT2 shRNA2 cells. Qualification of tumor weight in SW620/NC or SW620/GFPT2 shRNA1 or SW620/GFPT2 shRNA2 groups. B. Representative images of Ki67 staining in subcutaneous tumor sections by immunohistochemistry. Scale bars: 20 μm. Error bars represent mean ± SD from three independent experiments. *P<0.05.